JOURNAL OF AIRCRAFT
Vol. 43, No. 5, September–October 2006

Response of Composite Fuselage Sandwich Side Panels Subjected to Internal Pressure and Axial Tension

Marshall Rouse*
NASA Langley Research Center, Hampton, Virginia 23681
Damodar R. Ambur†
NASA Glenn Research Center, Cleveland, Ohio 44135
Bernard Dopker‡
Boeing Commercial Airplane Company, Seattle, Washington 98124
and
Bharat Shah§
Lockheed Martin Aeronautical Systems Company, Marietta, Georgia 30063

DOI: 10.2514/1.22397

An experimental and analytical study on the structural behavior of two carbon fiber reinforced plastic composite sandwich fuselage side panels for a transport aircraft is presented. Each panel has two window cutouts and three frames and uses a distinctly different structural concept. These panels have been evaluated with internal-pressure and axial tension load loading conditions. One of the sandwich panels was tested with the middle frame removed to demonstrate the suitability of this two-frame design for supporting the prescribed biaxial loading conditions with twice the initial frame spacing. A damage tolerance study was conducted on the two-frame panel by cutting a notch in the panel that originated at the edge of a cutout and extended in the panel hoop direction through the window-belt area. This panel with a notch was tested in a combined-load condition. Both sandwich panel designs successfully satisfied all desired load requirements in the experimental part of the study, and experimental results from the two-frame panel with and without damage are fully explained by the analytical results. The results of this study suggest that there is potential for using sandwich structural concepts with greater than usual frame spacing to further reduce aircraft fuselage structural weight.

I. Introduction

THE potential for cost and weight reduction offered by carbon fiber reinforced plastic (CFRP) composite-facesheet sandwich structures in aircraft fuselage side panels is currently being investigated in the airframe industry. Structural trade studies for sandwich concepts that use advanced material placement methods, such as tow placement for skin and three-dimensional braiding for frames, have identified a 25% cost and weight reduction compared to conventional integrally stiffened metallic structures ([1]). Sandwich structures offer additional potential for weight reduction by decreasing the number of frames by increasing the fuselage frame spacing. Sandwich structures are good candidates for implementing greater frame spacing than the usual 0.508 m (20 in.) to 0.509 m (22 in.) because skin panels for these structures have much higher bending stiffnesses than the more conventional stringer-frame stiffened skins with minimum gauge thicknesses. The sandwich panels described in the present paper use two proposed structural concepts and have been designed to generate preliminary performance information for sandwich structures. One of the panels has been tested with twice the usual fuselage frame spacing and a notch at the window-belt region.

Presented as Paper 1708 at the 38th AIAA/ASME/ASCE/AHS/ASC Structures, Structural Dynamics, and Materials Conference, Long Beach, California, 20–23 April 1998; received 13 January 2006; accepted for publication 10 February 2006.

*Senior Aerospace Engineer, Mechanics of Structures and Materials Branch, Senior Member AIAA.
†Chief, Materials and Structures Division, Associate Fellow AIAA.
‡Specialist Engineer, Technology and Product Development Group.
§Senior Staff Engineer, Advanced Structures and Materials Division, Associate Fellow AIAA.

An important aspect of designing aircraft structures is understanding the response of undamaged and damaged sandwich structures when they are subjected to combined-loading conditions that are representative of the actual operating flight environment. Very limited information currently exists for curved composite sandwich panels with damage at critical locations and subjected to combined-loading conditions. To understand better the structural behavior of a sandwich fuselage side panel with windows and with damage at a highly stressed location, biaxial tension tests have been performed by subjecting one of the damaged panels to internal-pressure loading conditions.

Finite element analyses were performed to predict the structural response of the sandwich panels assembled in the test machine and subjected to different test loading conditions. The experimental results and their correlation with the analytical results for the undamaged loading conditions are discussed in the present paper. The objective of this paper is to present experimental and analytical results of a CFRP composite sandwich fuselage panel subjected to internal pressure and axial loading. Also, the effect of damage on the structural behavior of the fuselage panels will be described.

II. Test Panels and Test Description

The sandwich fuselage panels considered in the present study have three circumferential frame and two window belts (three sets of vertical dashed lines and two sets of horizontal dashed lines shown in Fig. 1a, respectively). The panels have overall dimensions of 309.88-mm (122 in.) radius, 182.88-mm (72-in.) length, and 160.02-mm (63-in.) arc width. Each of these panels have two window cutouts, one located midway between the center frame and each of the outer frames. The elliptical window cutouts are 50.60-mm (19.92-in.) long in the fuselage circumferential direction and 38.86-mm (15.30-in.) long in the fuselage longitudinal direction.

The sandwich panel facesheets were fabricated from Hercules, Inc. AS4/8552 graphite-epoxy material and the core was made from a Hexcel Korex honeycomb material. The 0, 45, and 90° ply directions

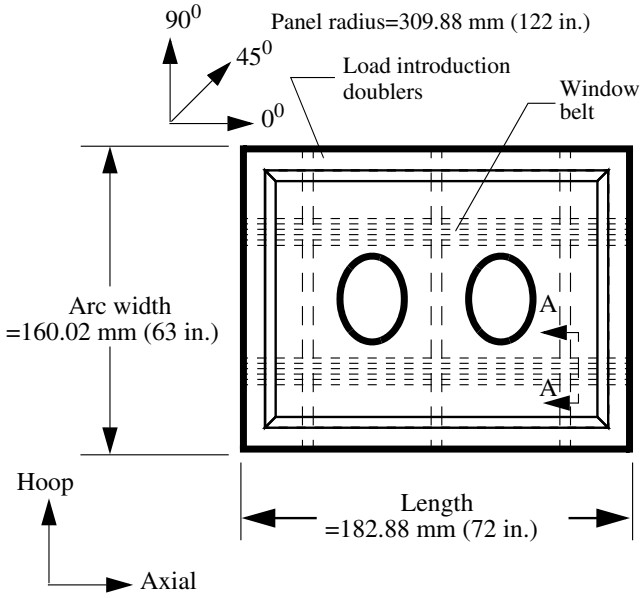

a) Plan view of the panel

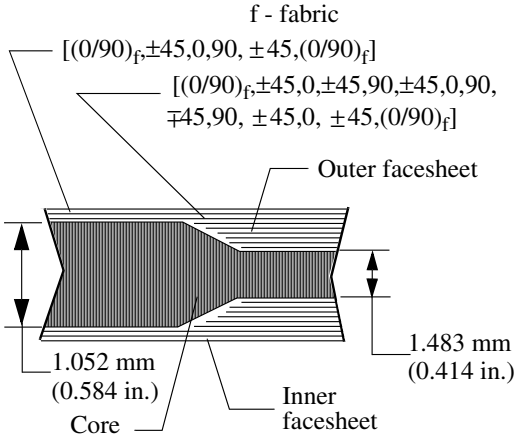

b) Panel 1 cross-sectional view of section AA

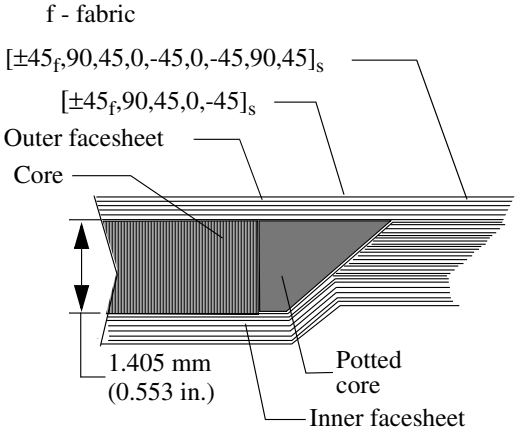

c) Panel 2 cross-sectional view

Fig. 1 Geometry, loading, and construction details for the sandwich panels.

are also indicated in Fig. 1a. The facesheet utilizes tow-placed inner plies and fabric outer layers. The fuselage frames and window frames were fabricated from fiber preforms consisting of triaxially braided AS4 graphite fibers impregnated with 3M Company PR500 epoxy resin using a resin transfer molding (RTM) process and autoclave

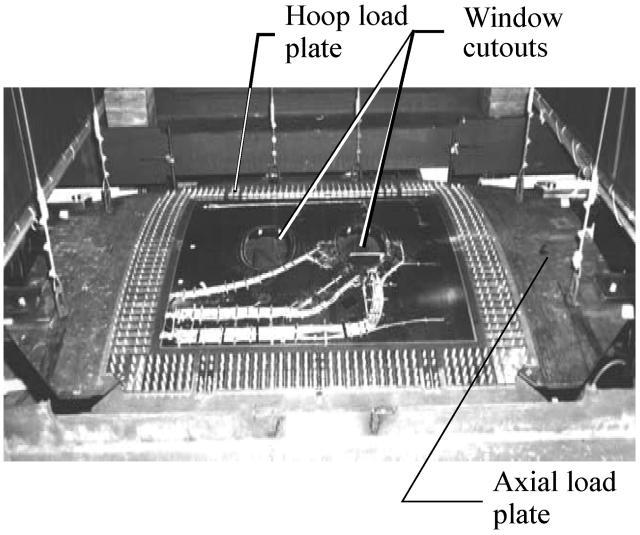

Fig. 2 Photograph of a sandwich panel assembly.

cured. The sandwich skin and the precured frames were cocured in a single stage. Typical material properties for the tow-placed, fabric, and triaxially braided AS4/8552 and AS4/PR500 graphite-epoxy material systems are presented in Table 1.

Typical construction details of the test panels are shown in Fig. 1 using cross-sectional views. The cross-sectional views in Figs. 1b and 1c illustrate details of the panels in the window region. For the panel 1 cross-sectional view in Fig. 1b, the sandwich core is contoured on both the concave and convex sides of the panel to accommodate ±45° plies added to the 8-ply-thick facesheet near the window region. When cured, the sandwich panel has a constant inner and outer mold line radius resulting in a uniform total thickness throughout the skin. The cross-sectional view shown in Fig. 1c illustrates details of the panel 2 window region. This sandwich panel is made of 18-ply facesheets and the sandwich core is terminated in the window region by tapering the core of the inner surface to form a 36-ply-thick laminate in the window region. The core is also potted with an epoxy closeout in the tapered region. When cured, sandwich panel 2 has a nonconstant inner mold line radius and a reduced skin thickness in the window region of the panel. For both panel concepts, graphite-epoxy doublers fabricated from preimpregnated fabric were cocured at the curved and flat edges of the panel to introduce the axial and hoop loads into the panel skin. A photograph of a test panel is shown in Fig. 2.

To evaluate the sandwich panel designs, combined-load tests were performed on the two undamaged panels in a pressure-box test machine ([2]). A schematic of the pressure-box test machine is shown in Fig. 3. The pressure-box test machine is capable of applying axial tensile loads of up to 1,225,888 N/m (7000 lb/in.) and internal-pressure loads of up to 0.138 MPa (20 psig). Axial loads are applied to the panel by two 1.01-N hydraulic actuators connected to a curved steel axial load plate located at each end of the panel. Internal pressure loading is applied to the concave side of the panel using a 0.689 MPa (100 psig) air supply source. Circumferentials of hoop loads that develop in the skin of the panel are reacted by an annular steel plate and two steel rods that are connected to each end of the three frames.

In the undamaged condition, panel 1 was subjected to design ultimate loading conditions of 0.125 MPa (18.2 psi) internal pressure with the corresponding bulkhead axial tension load of 194,391 N/m (1110 lb/in.); and a combined-load condition of 0.094 MPa (13.65 psi) of internal pressure and 285,457 N/m (2450 lb/in.) of axial tension. These same test conditions were also applied to panel 1 with its center frame removed to gather preliminary structural performance information for a panel with twice the initial frame spacing. A notch (machined damage) was then cut in panel 1 along the fuselage hoop direction starting at the window and extending through the window frame and the skin after testing in the undamaged condition. This damaged panel was then loaded to the

Table 1 Typical material properties for the graphite-epoxy materials used to manufacture the sandwich panel

Property	Tow AS4/8552	Fabric AS4/8552	Triaxially braid AS4/PR500	Korex core 4.5 lb, 1/8 in. cell
Longitudinal modulus, E_1 GPa (Msi)	11.470 (18.30)	5.767 (9.20)	4.701 (7.5)	0.0001 (0.0001)
Longitudinal modulus, E_2 GPa (Msi)	0.852 (1.36)	5.767 (9.20)	4.701 (7.5)	0.0001 (0.0001)
Lateral modulus, E_3 GPa (Msi)	0.852 (1.36)	0.815 (1.30)	——	0.0213 (0.0340)
In-plane shear modulus, G_{12} GPa (Msi)	0.476 (0.76)	0.451 (0.72)	0.357 (0.57)	0.0001 (0.0001)
Transverse shear modulus, G_{23} GPa (Msi)	0.326 (0.52)	0.313 (0.50)	0.251 (0.40)	0.0085 (0.0136)
Transverse shear modulus, G_{23} GPa (Msi)	0.476 (0.76)	0.313 (0.50)	0.357 (0.57)	0.0085 (0.0136)
Major Poisson's ratio, ν_{12}	0.32	0.04	0.29	0.30

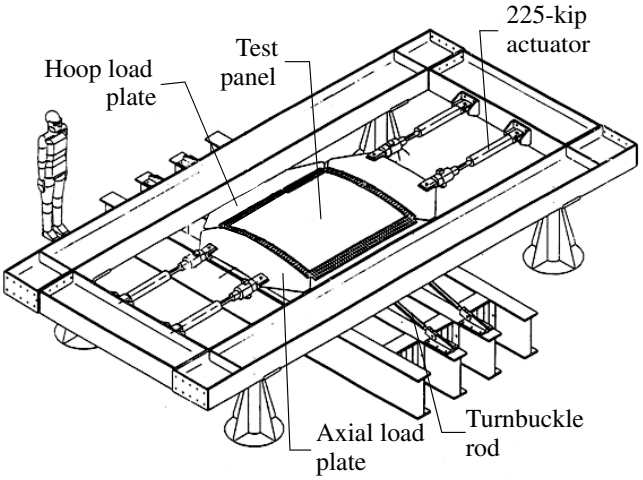

Fig. 3 Schematic of pressure-box test machine.

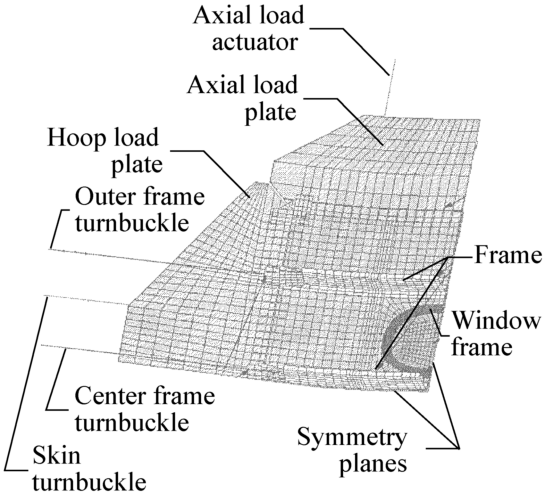

Fig. 4 Finite element model of a sandwich panel.

design limit load condition of 0.061 MPa (8.85 psi) of internal pressure and 285, 457 N/m (1630 lb/in.) of axial tension without failure. Panel 2 was subjected to design ultimate loading conditions of 0.125 MPa (18.2 psi) internal pressure with the corresponding bulkhead axial tension load of 194, 391 N/m (1110 lb/in.); and a combined-load condition of 0.094 MPa (13.65 psi) of internal pressure and 285, 457 N/m (2130 lb/in.) of axial tension. The panels were instrumented with electrical resistance strain gages on the outer and inner skin surfaces to record strains.

III. Finite Element Models

The finite element model of panel 1 in the pressure-box test machine is shown in Fig. 4 where symmetry has been exploited to reduce model size. The sandwich panel is modeled and analyzed using the ABAQUS finite element analysis program ([3]) with 4-node isoparametric elements for the facesheets and three 8-node solid elements through the thickness to represent the honeycomb core. These shell elements and solid elements have compatible translational displacement fields for the midsurface plane. The rotational freedoms of the shell element are not anticipated to cause significant issues when attached to the solid elements. The ply drop-offs in the facesheets are discretely modeled to represent the thickness changes appropriately. The circumferential frames and the window frames are modeled using 4-node shell elements. The window glazing is also modeled using shell elements. Only reaction forces along the edges perpendicular to the window glazing are transmitted to the window frame. It is assumed that no in-plane forces are transmitted to the panel by the window glazing.

The hoop and axial load introduction plates of the test fixture are modeled with shell elements. Because symmetry boundary conditions are assumed at the axial and hoop centerlines, only a quarter of the structure is modeled and analyzed. The quarter model of the test panel in the pressure box has a total of 5343 elements and approximately 26,650 degrees of freedom. Along the sandwich panel hoop direction, the test fixture hoop-load-reaction turnbuckles for the skin and frames are represented with the appropriate length and stiffnesses to model the panel boundary conditions properly. Axial load is applied to the beams representing the hydraulic actuators attached to the axial load introduction plates. Geometric nonlinear analyses have been performed for all load cases considered in the present paper. Finite element model details for panel 2 were identical to panel 1.

IV. Results and Discussion

The sandwich panels and the pressure-box test machine were modeled and analyzed for critical loading conditions to determine the panel response both with and without damage. The analytical results are compared with the experimental results in this section.

A. Undamaged Panel Results

1. Combined 0.125 MPa (18.2 psi) Internal Pressure and 194, 391 *N/m (*1110 *lb/in.) Axial Loading Condition*

The panel 1 outer surface hoop and axial strain variations along the elliptical cutout edge obtained from the finite element analysis for this loading condition are presented in Fig. 5. The hoop strain has the largest positive value at the edge of the elliptical cutout near the minor axis and the largest negative value along the major axis. The axial strain results in Fig. 5b indicate a large positive strain value at the edge of the elliptical cutout at the ellipse major axis and a small negative value at the boundary of the cutout at its minor axis. The finite element analytical results in Fig. 5 are consistent with the experimental results presented in Fig. 6. The data points presented in Fig. 6a correspond to strain gauge locations indicated in Fig. 6b with $a = 0°\square$, 30°, 45°, 60°, and 90°. For the panel outer surface, the measured axial strain values at the minor axis is -1000 μm/m and the value at the major axis is 2200 μm/m. The finite element analytical results at the corresponding locations are -662 and 1420 μm/m, respectively. The analytical strain concentration factor for the axial stress is 3.1 for this loading condition based on a far-field strain value away from the cutout of 460 μm/m.

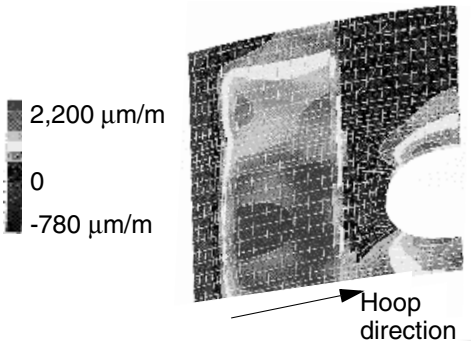

a) Hoop strain contour results

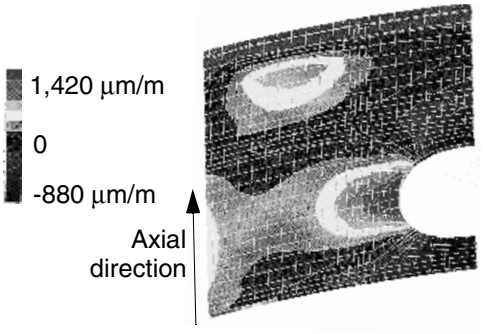

b) Axial strain contour results

Fig. 5 Finite element analysis results for panel 1 (three-frame) outer surface for a combined 0.125 MPa (18.2 psi) internal pressure and 1110 lb/in (finite element model of fixture not shown).

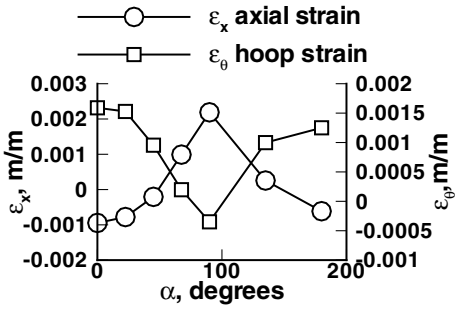

a) Axial and hoop strain near edge of elliptical cutout

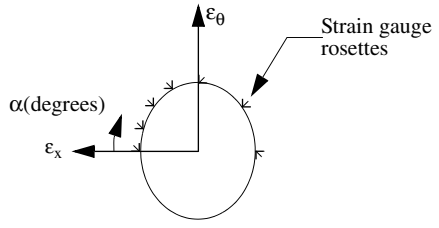

b) Strain gage locations near edge of elliptical cutout

Fig. 6 Experimental strain results for panel 1 (three-frame) outer surface for a combined 0.125 MPa (18.2 psi) internal pressure and 194, 391 N/m (1110 lb/in.) axial loading condition.

The analytical strain results for panel 2 for this loading condition are presented in Fig. 7. The analytical strains for the hoop strains are −272 and 1730 μm/m at the edge of the cutout along the major and minor axes, respectively. The axial strains shown in Fig. 7b provide analytical estimates for axial strains to be 1190 and −969 μm/m at the edge of the cutout along the major and minor axes of the ellipse, respectively. The experimental results for this loading case are presented in Fig. 8, which suggests good comparisons with analytical

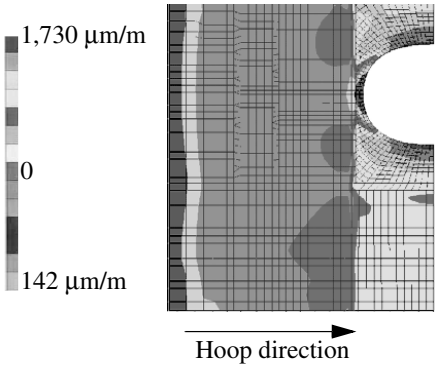

a) Hoop strain contours results

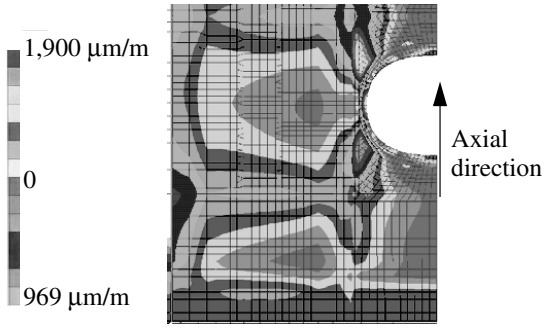

b) Axial strain contour results

Fig. 7 Finite element analysis results for panel 2 (three-frame) outer surface for a combined 0.125 MPa (18.2 psi) internal pressure and 194, 391 N/m (1110 lb/in.) axial loading condition.

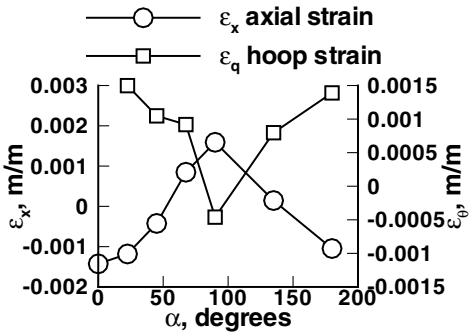

Fig. 8 Experimental axial and hoop strain results on panel 2 (three-frame) outer surface for a combined 0.125 MPa (18.2 psi) internal pressure and 194, 391 N/m (1110 lb/in.) axial loading condition.

results. The trends for strain distribution are very similar to those for panel 1, although panel 2 strains are lower than panel 1 strains.

2. Combined 0.094 MPa (13.65 psi) Internal Pressure and 285, 457 N/m (2450 lb/in.) Axial Loading Condition

This test condition corresponds to the design ultimate loading condition with 0.094 MPa (13.65 psi) of internal pressure and 285, 457 N/m (2450 lb/in.) of axial loading. Panel 1 outer surface hoop and axial strain results from the finite element analysis are presented in Fig. 9. These analytical results suggest that the hoop strain has a small negative value along the cutout boundary at the ellipse's major axis and changes to a positive value at the ellipse's minor axis. The axial strain magnitudes are much larger than the hoop strains and are positive at the major axis and negative at the minor axis. The hoop and axial strain distributions from the experiment are presented in Fig. 10. The trends of the experimental results agree extremely well with the finite element analytical results. The experimentally measured strains on the panel outer surface in the hoop direction vary from 1150 to −900 μm/m compared to the

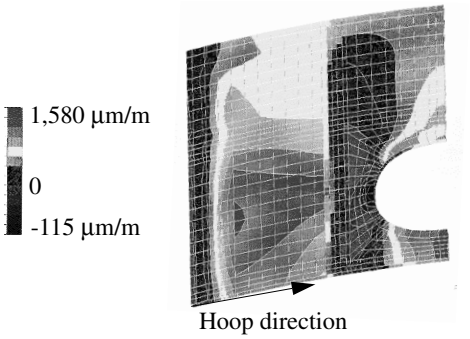

a) Hoop strain contour results

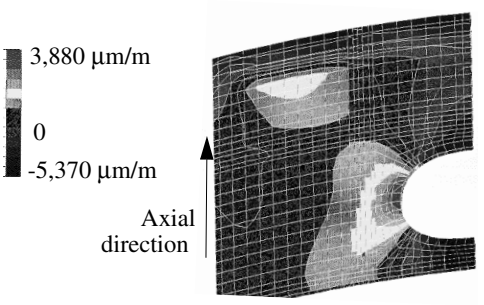

b) Axial strain contour results

Fig. 9 Panel 1 finite element analysis results for panel 1 (three-frame) outer surface for a combined 0.094 MPa (13.65 psi) internal pressure and 285, 457 N/m (2450 lb/in.) axial loading condition.

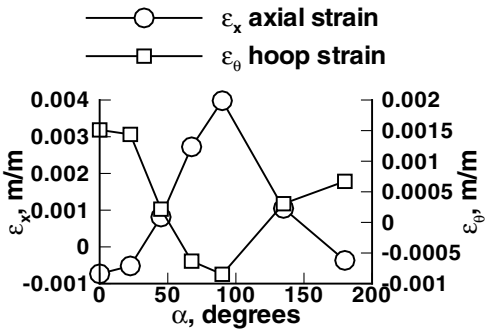

Fig. 10 Experimental axial and hoop strain results for panel 1 (three-frame) for a combined 0.094 MPa (13.65 psi) internal pressure and 285, 457 N/m (2450 lb/in.) axial loading condition.

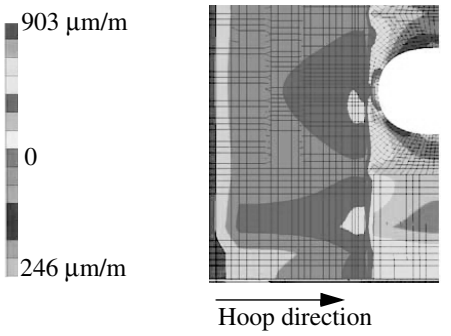

a) Hoop strain contour results

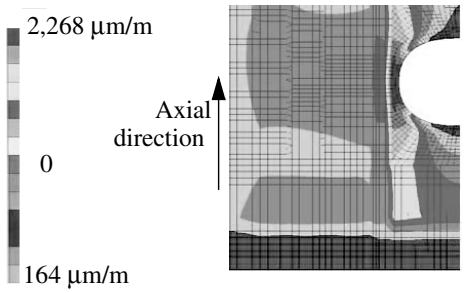

b) Axial strain contour results

Fig. 11 Finite element analysis results for panel 2 (three-frame) outer surface for a combined 0.094 MPa (13.65 psi) internal pressure and 285, 457 N/m (2130 lb/in.) axial loading condition.

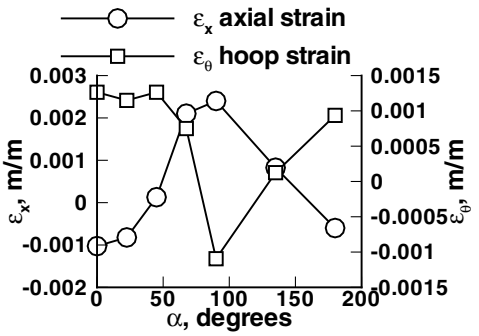

Fig. 12 Experimental axial and hoop strain results for panel 2 (three-frame) outer surface for a combined 0.094 MPa (13.65 psi) internal pressure and 285, 457 N/m (2130 lb/in.) axial loading condition.

finite element analytical results which vary from 937 to -949 μm/m In the axial direction, the measured strains vary from 4000 to -775 μm/m The corresponding results from the finite element analysis vary from 3540 to -815 μm/m.

The analytical strain results for panel 2 are presented in Fig. 11. The axial loading condition for this panel was limited to 285, 457 N/m (2130 lb/in.) The trends for hoop and axial strain results agree with the results for panel 1 very closely. The analytical strains for the hoop strains are 246 and 903 μm/m at the edge of the cutout along the major and minor axes, respectively. The axial strains shown in Fig. 11b provide analytical estimates for axial strains to be 2268 and -164 μm/m at the edge of the cutout along the major and minor axes of the ellipse, respectively. The experimental results for this loading case are presented in Fig. 12, which have trends that agree well with the experimental results. The hoop strain magnitudes for panel 2 are comparable to panel 1 strains for this load condition, whereas the maximum value for the axial strain along the major axis of the elliptical cutout is smaller by a factor of 2. The difference in axial strain is due to the tapering in the region of the cutout panel 2 to a laminate that has more 90° plies than panel 1.

Neither of the previous two loading conditions resulted in strain magnitudes that exceed the strain allowable of 4000 μm/m for the material systems used for manufacturing the test panels. The observed strain results for panel 2 suggest that, to have a response comparable to panel 1, this structural concept can be further sized to reduce its structural weight. There were no other indications from the experiment that suggested test panel failure. Further testing was conducted only on panel 1. After visual inspection, panel 1 was in pristine condition at the end of all the previous tests.

B. Panel 1 with the Center Frame Removed

The next set of loading conditions was imposed on panel 1 with the center frame removed. The objective of these tests was to gather preliminary information on the sandwich panel response with a frame spacing increased to 40.0 in. The frame was removed by severing the frame web above the frame attachment flange at the skin. The finite element analysis and experimental results corresponding to two loading conditions for this panel configuration are presented next.

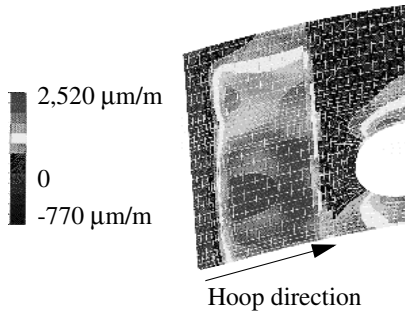

a) Hoop strain contour results

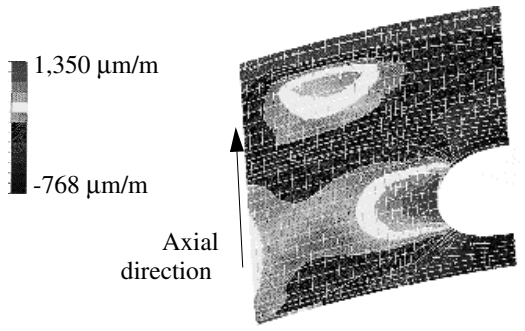

b) Axial strain contour results

Fig. 13 Finite element analysis results for panel 1 (two-frame) outer surface for a combined 0.125 MPa (18.2 psi) internal pressure and 194, 391 N/m (1110 lb/in.) axial loading condition.

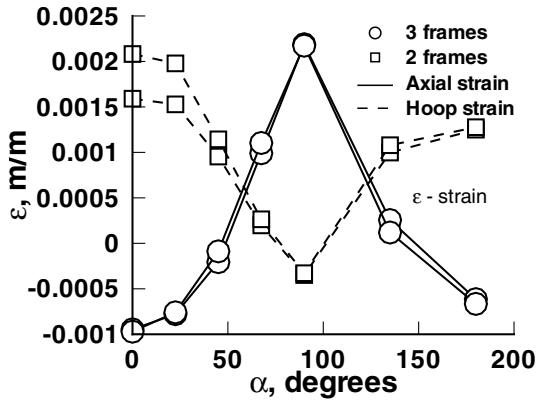

Fig. 14 Experimental axial and hoop strain results for panel 1 (two-frame) outer surface for a combined 0.125 MPa (18.2 psi) internal pressure and 194, 391 N/m (1110 lb/in.) axial loading condition.

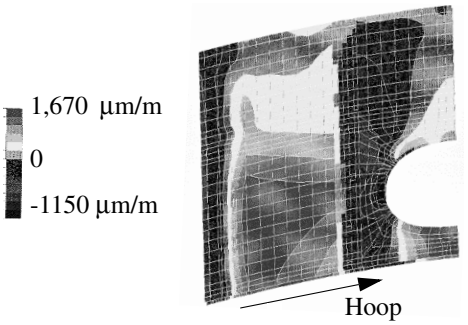

a) Hoop strain contour results

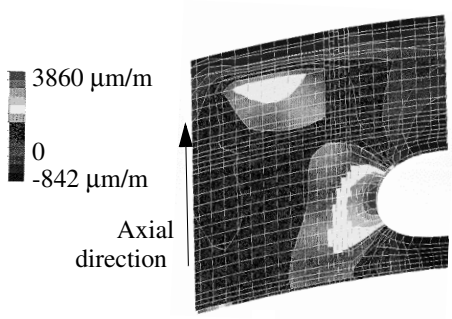

b) Axial strain contour results

Fig. 15 Finite element analysis results for panel 1 (two-frame) outer surface for a combined 0.094 MPa (13.65 psi) internal pressure and 285, 457 N/m (2450 lb/in.) axial loading condition.

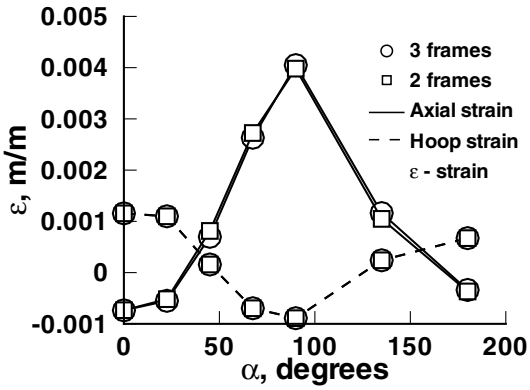

Fig. 16 Experimental axial and hoop strain results for panel 1 (two-frame) outer surface for a combined 0.094 MPa (13.65 psi) internal pressure and 285, 457 N/m (2450 lb/in.) axial loading condition.

1. Combined 0.125 MPa (18.2 psi) Internal Pressure and 194, 391 *N/m (*1110 *lb/in.) Axial Loading Condition*

The finite element analytical results for this loading condition are presented in Fig. 13. The hoop and axial surface strains are presented in Fig. 13 for the outer facesheet. The test was conducted by redistributing the loads in the severed frame to the remaining two frames to ensure that the panel was evaluated for the same load ratio of 80 and 20% of the load in the skin and the frames, respectively, for a given loading condition. The frame load for the panel with the two-frame configuration is greater than the frame load for the panel with the three-frame configuration. This increase in frame load is indicated by comparison of experimental results for the two-frame panel presented in Fig. 14 with the results for the three-frame panel in Fig. 6. The hoop strain in the remaining two frames increases by approximately 25% and the hoop strain in the skin between the two cutouts increases by approximately 12% due to the severing of the center frame. This increase in skin hoop strain is due to bending of the unsupported skin between the cutouts. The outer facesheet hoop strains from the experiment vary from approximately −400 to 2200 μm/m compared to the finite element results which vary from −770 to 2010 μm/m The axial strain results for this panel configuration corresponding to this loading condition are very similar to those for the panel with a three-frame configuration.

2. Combined 0.094 MPa (13.65 psi) Internal Pressure and 285, 457 *N/m (*2450 *lb/in.) Axial Loading Condition*

The panel outer surface hoop and axial strain results from finite element analysis are presented in Fig. 15 for this loading condition. The overall observations for the axial and hoop strains for this loading condition are very similar to the previous loading condition for the two-frame panel. The experimental strain results for the two-frame panel are compared with the three-frame panel results in Fig. 16. The maximum experimental axial strain along the cutout for the two-frame panel varies from −850 to 4000 μm/m compared to the analytical results which vary from −542 to 3860 μm/m. These strain magnitudes are comparable to the axial strains for the three-frame panel for the same loading condition. Bending of the skin between the frames is also observed for this loading condition and is

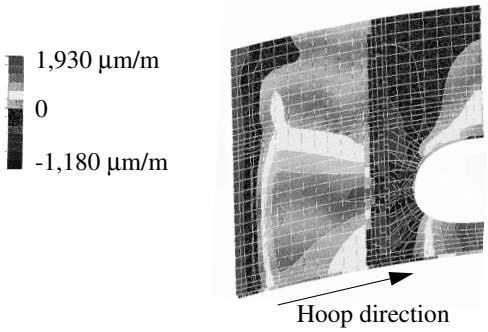

a) Hoop strain contour results

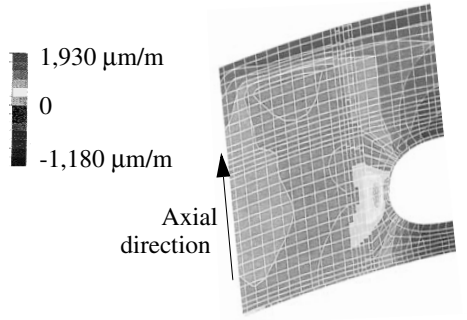

b) Axial strain contour results

Fig. 17 Finite element analysis results for the notched two-frame panel (panel 1) outer surface for a combined 0.061 MPa (8.85 psi) internal pressure and 1630 lb/in. axial loading condition.

similar to that observed for the previous loading condition for the two-frame panel.

The panel with the two-frame configuration responds in a predictable manner and the strain magnitudes for this loading condition are well within the strain allowables for failure initiation.

3. Panel 1 with Center Frame Removed and a Notch at One Cutout

The final test case considered in the present study was panel 1 with a center frame removed and a notch at one cutout. A maximum value for the undamaged test panel axial strain occurs at the edge of the elliptical cutout's major axis. The magnitude of the maximum strain is 4000 μm/m for the combined 0.094 MPa (13.65 psi) internal pressure and 285, 457 N/m (2450 lb/in.) axial loading condition. Damage in the form of a 1-in.-long saw-cut notch was inflicted at this critical location to study the damage tolerance of this sandwich panel concept with a combined-loading condition of 0.061 MPa (8.85 psi) internal pressure and 285, 457 N/m (1630 lb/in.) of axial load. This loading condition corresponds to 2/3 of the design ultimate loading condition. The notch was machined into the panel to extend in the panel hoop direction slightly beyond the window frame edge. The panel outer surface hoop and axial strain results from the finite element analysis for this combined-loading condition are presented in Fig. 17. The hoop strain for this loading condition varies from -1100 μm/m at $\alpha = 90°$ to 1900 μm/m at $\theta = 0°$ (refer to Fig. 6a). The strain magnitudes are higher for this loading condition than for the hoop strain results presented in Fig. 15 for the combined-loading condition with 0.094 MPa (13.65 psi) of internal pressure and 285, 457 N/m (2450 lb/in.) of axial loading which are 66% lower. The notch causes more panel bending in the skin between the two cutouts in this test case, causing the increase in strain. The axial strain results from the finite element analysis for the outer surface indicate that a maximum strain of approximately 5200 μm/m occurs at the tip of the machined notch. The experimental strain results for this load case are presented in Fig. 18. The axial strain results vary from -500 to 5800 μm/m and compare very well with the analytical results. No growth in the notch length was observed during the test.

The experimental hoop strain results along the length for the three-frame panel, for the two-frame panel, and for the two-frame panel with a notch at the window cutout region are compared in Fig. 19.

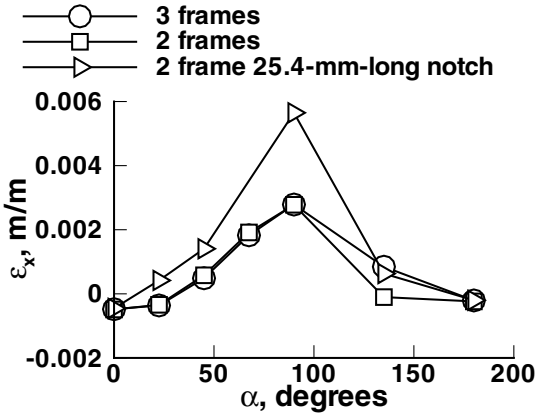

Fig. 18 Experimental axial strain results for the notched two-frame panel (panel 1) outer surface for a combined 0.125 MPa (8.85 psig) internal pressure and 285, 457 N/m (1630 lb/in.) axial loading condition.

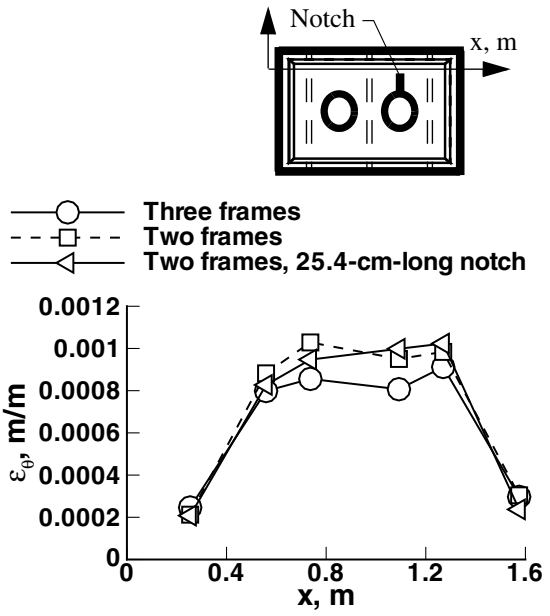

Fig. 19 Comparison of experimental far-field outer surface hoop strain results for panel 1 with three frames, two frames, and two frames with a notch for a combined 0.125 MPa (8.85 psig) internal pressure and 285, 457 N/m (1630 lb/in.) axial loading condition.

These results along the x axis suggest that the far-field strains in the hoop direction are influenced more by the removal of the frame than by the introduction of the notch. The increase in the panel strain state due to the introduction of the notch is local and does not result in any significant load redistribution.

V. Concluding Remarks

The response of two composite sandwich fuselage side panels with two window cutouts has been evaluated for internal pressure and axial tension. The panels have been tested in a three-frame configuration with combined-loading conditions that are representative of the design limit load and design ultimate load conditions. The strain magnitudes around the cutouts on the outer surfaces of the test panels for these loading conditions are within the design ultimate strain allowable value of 4000 μm/m for the material, suggesting that the structure satisfies the design requirements. The test results for panel 2 also indicate that, to get a response comparable to panel 1, panel 2 could be redesigned to achieve additional structure weight benefits. Examining data trends and magnitude indicates that the

finite element analytical results compare very well with the experimental results.

For a panel with a two-frame configuration, the finite element analytical and experimental results correlate well and the strain results are less than the ultimate strain allowables for the material. The damage tolerance of the panel with a two-frame configuration is also demonstrated by testing the panel at design limit load conditions with a notch at a window cutout region that is in the location of the highest value of axial stress. For this case, the maximum value for the axial strain obtained from the test and from the analysis is approximately 5200 μm/m with no growth in the notch length. This result suggests that the panel with twice the original frame spacing is capable of sustaining the design ultimate load conditions without damage and of sustaining the design limit load conditions with a 1-in.-long notch. This finding from the experiments is significant considering that reducing the number of frames results in a lighter weight structure. Based on the experimental results of both design concepts, lower stiffness at the window cutout area in panel 2 design, considerably lower critical axial strains were observed than for the panel 1 design. In summary, sandwich panels that are representative of aircraft fuselage structures with windows can be designed for minimum weight while meeting strict strength and damage tolerance criteria.

References

[1] Rouse, M., and Ambur, D. R., "Evaluation of Damaged and Undamaged Fuselage Panel Responses Subjected to Internal Pressure and Axial Load," *Proceedings of the Sixth NASA/DoD ACT Conference*, NASA, Anaheim, CA, 1995.

[2] Rouse, M., and Ambur, D. R., "Fuselage Response Simulation of Stiffened Panels Using a Pressure-box Test Machine," AIAA AIAA-95-1362-CP, April 1995.

[3] Anon, *ABAQUS Finite Element Code*, Hibbitt, Karlsson and Sorensen, Inc., Pawtucket, RI, Vols. 1–2, 1995.